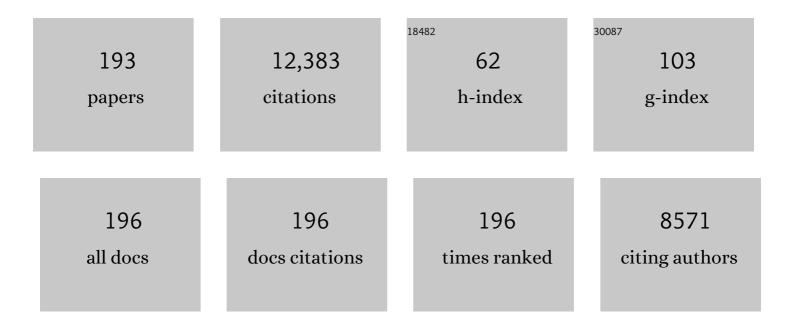
Manfred R Strecker

List of Publications by Year in descending order

Source: https://exaly.com/author-pdf/5244497/publications.pdf Version: 2024-02-01



#	Article	IF	CITATIONS
1	Spatially variable response of Himalayan glaciers to climate change affected by debris cover. Nature Geoscience, 2011, 4, 156-159.	12.9	812
2	Late Cenozoic Moisture History of East Africa. Science, 2005, 309, 2051-2053.	12.6	328
3	Late Quaternary intensified monsoon phases control landscape evolution in the northwest Himalaya. Geology, 2005, 33, 149.	4.4	319
4	High- and low-latitude forcing of Plio-Pleistocene East African climate and human evolution. Journal of Human Evolution, 2007, 53, 475-486.	2.6	287
5	Glacier-surface velocities in alpine terrain from optical satellite imagery—Accuracy improvement and quality assessment. Remote Sensing of Environment, 2008, 112, 3806-3819.	11.0	286
6	Orographic barriers, highâ€resolution TRMM rainfall, and relief variations along the eastern Andes. Geophysical Research Letters, 2008, 35, .	4.0	275
7	Climatic control on rapid exhumation along the Southern Himalayan Front. Earth and Planetary Science Letters, 2004, 222, 791-806.	4.4	263
8	Arabia-Eurasia continental collision: Insights from late Tertiary foreland-basin evolution in the Alborz Mountains, northern Iran. Bulletin of the Geological Society of America, 2011, 123, 106-131.	3.3	244
9	Abnormal monsoon years and their control on erosion and sediment flux in the high, arid northwest Himalaya. Earth and Planetary Science Letters, 2005, 231, 131-146.	4.4	219
10	Human evolution in a variable environment: the amplifier lakes of Eastern Africa. Quaternary Science Reviews, 2010, 29, 2981-2988.	3.0	196
11	Spatiotemporal trends in erosion rates across a pronounced rainfall gradient: Examples from the southern Central Andes. Earth and Planetary Science Letters, 2012, 327-328, 97-110.	4.4	183
12	Low slip rates and long-term preservation of geomorphic features in Central Asia. Nature, 2002, 417, 428-432.	27.8	180
13	Segmentation of megathrust rupture zones from foreâ€arc deformation patterns over hundreds to millions of years, Arauco peninsula, Chile. Journal of Geophysical Research, 2009, 114, .	3.3	167
14	Analysis of partially emerged corals and reef terraces in the central Vanuatu Arc: Comparison of contemporary coseismic and nonseismic with quaternary vertical movements. Journal of Geophysical Research, 1987, 92, 4905-4933.	3.3	164
15	Late Cenozoic tectonism, collapse caldera and plateau formation in the central Andes. Earth and Planetary Science Letters, 2001, 188, 299-311.	4.4	164
16	Climatic forcing of asymmetric orogenic evolution in the Eastern Cordillera of Colombia. Bulletin of the Geological Society of America, 2008, 120, 930-949.	3.3	155
17	East African climate change and orbital forcing during the last 175 kyr BP. Earth and Planetary Science Letters, 2003, 206, 297-313.	4.4	152
18	Late Cenozoic tectonic development of the intramontane Alai Valley, (Pamir-Tien Shan region, central) Tj ETQq0 C) 0 rgBT /0 2.8	Dverlock 10 T 142

21, 3-1-3-19.

#	Article	IF	CITATIONS
19	Tectonic control on ¹⁰ Beâ€derived erosion rates in the Garhwal Himalaya, India. Journal of Geophysical Research F: Earth Surface, 2014, 119, 83-105.	2.8	141
20	Uplift, exhumation and precipitation: tectonic and climatic control of Late Cenozoic landscape evolution in the northern Sierras Pampeanas, Argentina. Basin Research, 2003, 15, 431-451.	2.7	140
21	Late Cenozoic tectonism and landscape development in the foreland of the Andes: Northern Sierras Pampeanas (26°–28°S), Argentina. Tectonics, 1989, 8, 517-534.	2.8	139
22	Rotation of extension direction in the central Kenya Rift. Geology, 1990, 18, 299.	4.4	135
23	Cenozoic contractional reactivation of Mesozoic extensional structures in the Eastern Cordillera of Colombia. Tectonics, 2006, 25, n/a-n/a.	2.8	133
24	Late Miocene–Pliocene deceleration of dextral slip between Pamir and Tarim: Implications for Pamir orogenesis. Earth and Planetary Science Letters, 2011, 304, 369-378.	4.4	133
25	Oceanic-style subduction controls late Cenozoic deformation of the Northern Pamir orogen. Earth and Planetary Science Letters, 2013, 363, 204-218.	4.4	131
26	Climate change in response to orographic barrier uplift: Paleosol and stable isotope evidence from the late Neogene Santa MarÃa basin, northwestern Argentina. Bulletin of the Geological Society of America, 2001, 113, 728-742.	3.3	130
27	Multiple landslide clusters record Quaternary climate changes in the northwestern Argentine Andes. Palaeogeography, Palaeoclimatology, Palaeoecology, 2003, 194, 109-121.	2.3	128
28	Quaternary deformation in the Eastern Pamirs, Tadzhikistan and Kyrgyzstan. Tectonics, 1995, 14, 1061-1079.	2.8	124
29	Propagation of orographic barriers along an active range front: insights from sandstone petrography and detrital apatite fission-track thermochronology in the intramontane Angastaco basin, NW Argentina. Basin Research, 2006, 18, 1-26.	2.7	118
30	Dome formation and extension in the Tethyan Himalaya, Leo Pargil, northwest India. Bulletin of the Geological Society of America, 2006, 118, 635-650.	3.3	117
31	Accommodation of transpressional strain in the Arabiaâ€Eurasia collision zone: new constraints from (Uâ€Th)/He thermochronology in the Alborz mountains, north Iran. Tectonics, 2013, 32, 1-18.	2.8	114
32	Coastal deformation and great subduction earthquakes, Isla Santa Maria, Chile (37ÂS). Bulletin of the Geological Society of America, 2006, 118, 1463-1480.	3.3	109
33	Climate change and mass movements in the NW Argentine Andes. Earth and Planetary Science Letters, 2000, 179, 243-256.	4.4	108
34	Orogenic wedge advance in the northern Andes: Evidence from the Oligocene-Miocene sedimentary record of the Medina Basin, Eastern Cordillera, Colombia. Bulletin of the Geological Society of America, 2009, 121, 780-800.	3.3	106
35	Late Miocene climate variability and surface elevation in the central Andes. Earth and Planetary Science Letters, 2010, 290, 173-182.	4.4	106
36	Structural and lithological controls on large Quaternary rock avalanches (sturzstroms) in arid northwestern Argentina. Bulletin of the Geological Society of America, 1999, 111, 934-948.	3.3	105

#	Article	IF	CITATIONS
37	Response of intracontinental deformation in the central Andes to late Cenozoic reorganization of South American Plate motions. Tectonics, 2000, 19, 452-467.	2.8	104
38	From tectonically to erosionally controlled development of the Himalayan orogen. Geology, 2005, 33, 689-692.	4.4	104
39	Processes of oscillatory basin filling and excavation in a tectonically active orogen: Quebrada del Toro Basin, NW Argentina. Bulletin of the Geological Society of America, 2005, 117, 887.	3.3	101
40	Stress field changes in the Afro-Arabian rift system during the Miocene to Recent period. Tectonophysics, 1997, 278, 47-62.	2.2	98
41	Erosional variability along the northwest Himalaya. Journal of Geophysical Research, 2009, 114, .	3.3	94
42	Neotectonics and catastrophic failure of mountain fronts in the southern intra-Andean Puna Plateau, Argentina. Geology, 2001, 29, 619.	4.4	89
43	Seismotectonic range-front segmentation and mountain-belt growth in the Pamir-Alai region, Kyrgyzstan (India-Eurasia collision zone). Bulletin of the Geological Society of America, 1999, 111, 1665.	3.3	88
44	Middle to late Miocene Middle Eastern climate from stable oxygen and carbon isotope data, southern Alborz mountains, N Iran. Earth and Planetary Science Letters, 2010, 300, 125-138.	4.4	88
45	The role of inherited extensional fault segmentation and linkage in contractional orogenesis: a reconstruction of Lower Cretaceous inverted rift basins in the Eastern Cordillera of Colombia. Basin Research, 2009, 21, 111-137.	2.7	87
46	Neogene to Quaternary broken foreland formation and sedimentation dynamics in the Andes of NW Argentina (25°S). Tectonics, 2011, 30, .	2.8	86
47	Increased sediment accumulation rates and climatic forcing in the central Andes during the late Miocene. Geology, 2007, 35, 979.	4.4	85
48	Steady state erosion of critical Coulomb wedges with applications to Taiwan and the Himalaya. Journal of Geophysical Research, 2004, 109, .	3.3	83
49	Early anthropogenic impact on Western Central African rainforests 2,600 y ago. Proceedings of the National Academy of Sciences of the United States of America, 2018, 115, 3261-3266.	7.1	83
50	Timing and extent of late Quaternary glaciation in the western Himalaya constrained by 10Be moraine dating in Garhwal, India. Quaternary Science Reviews, 2010, 29, 815-831.	3.0	82
51	Late Pleistocene–Holocene rise and collapse of Lake Suguta, northern Kenya Rift. Quaternary Science Reviews, 2009, 28, 911-925.	3.0	81
52	Formation of landslide-dammed lakes during a wet period between 40,000 and 25,000 yr B.P. in northwestern Argentina. Palaeogeography, Palaeoclimatology, Palaeoecology, 1999, 153, 277-287.	2.3	80
53	Fragmentation of a foreland basin in response to out-of-sequence basement uplifts and structural reactivation: El Cajon-Campo del Arenal basin, NW Argentina. Bulletin of the Geological Society of America, 2007, 119, 637-653.	3.3	80
54	From tectonically to erosionally controlled development of the Himalayan orogen. Geology, 2005, 33, 689.	4.4	77

#	Article	IF	CITATIONS
55	Evidence for middle Miocene uplift of the East African Plateau. Geology, 2010, 38, 543-546.	4.4	76
56	Implications of the fault scaling law for the growth of topography: mountain ranges in the broken foreland of north-east Tibet. Terra Nova, 2004, 16, 157-162.	2.1	75
57	Precipitation evolution of Central Asia during the last 5000 years. Holocene, 2017, 27, 142-154.	1.7	75
58	Unsteady evolution of the Bolivian Subandean thrust belt: The role of enhanced erosion and clastic wedge progradation. Earth and Planetary Science Letters, 2009, 281, 134-146.	4.4	74
59	Can stable isotopes ride out the storms? The role of convection for water isotopes in models, records, and paleoaltimetry studies in the central Andes. Earth and Planetary Science Letters, 2014, 407, 187-195.	4.4	72
60	Average Pleistocene Climatic Patterns in the Southern Central Andes: Controls on Mountain Glaciation and Paleoclimate Implications. Journal of Geology, 2002, 110, 211-226.	1.4	69
61	Middle Eoceneâ€Oligocene brokenâ€foreland evolution in the Andean Calchaqui Valley, NW Argentina: insights from stratigraphic, structural and provenance studies. Basin Research, 2013, 25, 574-593.	2.7	68
62	Increased late Pleistocene erosion rates during fluvial aggradation in the Garhwal Himalaya, northern India. Earth and Planetary Science Letters, 2015, 428, 255-266.	4.4	67
63	Late Neogene and active orogenic uplift in the Central Pontides associated with the North Anatolian Fault: Implications for the northern margin of the Central Anatolian Plateau, Turkey. Tectonics, 2011, 30, .	2.8	66
64	Using uplifted Holocene beach berms for paleoseismic analysis on the Santa MarÃa Island, south-central Chile. Geophysical Research Letters, 2006, 33, .	4.0	63
65	A 17-My-old whale constrains onset of uplift and climate change in east Africa. Proceedings of the National Academy of Sciences of the United States of America, 2015, 112, 3910-3915.	7.1	61
66	Tephrochronologic Constraints on Temporal Distribution of Large Landslides in Northwest Argentina. Journal of Geology, 2000, 108, 35-52.	1.4	59
67	100 kyr fluvial cut-and-fill terrace cycles since the Middle Pleistocene in the southern Central Andes, NW Argentina. Earth and Planetary Science Letters, 2017, 473, 141-153.	4.4	59
68	Late Cenozoic extension and crustal doming in the Indiaâ€Eurasia collision zone: New thermochronologic constraints from the NE Chinese Pamir. Tectonics, 2013, 32, 763-779.	2.8	58
69	Effect of vegetation cover on millennial-scale landscape denudation rates in East Africa. Lithosphere, 2015, 7, 408-420.	1.4	58
70	Differential structural and geomorphic mountain-front evolution in an active continental collision zone: The northwest Pamir, southern Kyrgyzstan. Bulletin of the Geological Society of America, 2003, 115, 166-181.	3.3	57
71	Mechanics and erosion of basement-cored uplift provinces. Journal of Geophysical Research, 2005, 110,	3.3	57
72	Dynamics of deformation and sedimentation in the northern Sierras Pampeanas: An integrated study of the Neogene Fiambala basin, NW Argentina. Bulletin of the Geological Society of America, 2008, 120, 1518-1543.	3.3	55

#	Article	IF	CITATIONS
73	Fault-kinematic and geomorphic observations along the North Tehran Thrust and Mosha Fasham Fault, Alborz mountains Iran: implications for fault-system evolution and interaction in a changing tectonic regime. Geophysical Journal International, 2009, 177, 676-690.	2.4	54
74	Large surface velocity fluctuations of Biafo Glacier, central Karakoram, at high spatial and temporal resolution from optical satellite images. Journal of Glaciology, 2012, 58, 569-580.	2.2	53
75	Kinematic evolution of fault ramps and its role in development of landslides and lakes in the northwestern Argentine Andes. Geology, 1999, 27, 307.	4.4	52
76	Late Mozambique Belt structures in western Kenya and their influence on the evolution of the Cenozoic Kenya Rift. Journal of Structural Geology, 1994, 16, 189-201.	2.3	51
77	Orthogonal to oblique rifting: effect of rift basin orientation in the evolution of the North basin, Malawi Rift, East Africa. Basin Research, 2007, 19, 393-407.	2.7	51
78	Role of climate and vegetation density in modulating denudation rates in the Himalaya. Earth and Planetary Science Letters, 2016, 445, 57-67.	4.4	51
79	Morphotectonic segmentation of an active forearc, 37°–41°S, Chile. Geomorphology, 2008, 94, 98-116.	2.6	50
80	Normal faulting along the southern margin of the Puna Plateau, northwest Argentina. Tectonics, 2009, 28, .	2.8	50
81	Tectonic controls on Cenozoic foreland basin development in the northâ€eastern Andes, Colombia. Basin Research, 2010, 22, 874-903.	2.7	50
82	Segmentation of the 2010 Maule Chile earthquake rupture from a joint analysis of uplifted marine terraces and seismic-cycle deformation patterns. Quaternary Science Reviews, 2015, 113, 171-192.	3.0	50
83	Climate-driven sediment aggradation and incision since the late Pleistocene in the NW Himalaya, India. Earth and Planetary Science Letters, 2016, 449, 321-331.	4.4	50
84	Neotectonic basin and landscape evolution in the Eastern Cordillera of <scp>NW</scp> Argentina, Humahuaca Basin (~24°S). Basin Research, 2013, 25, 554-573.	2.7	48
85	The growth of a mountain belt forced by base-level fall: Tectonics and surface processes during the evolution of the Alborz Mountains, N Iran. Earth and Planetary Science Letters, 2015, 425, 204-218.	4.4	47
86	The Kenya rift revisited: insights into lithospheric strength through data-driven 3-D gravity and thermal modelling. Solid Earth, 2017, 8, 45-81.	2.8	47
87	Differential uplift along the northern margin of the Central Anatolian Plateau: inferences from marine terraces. Quaternary Science Reviews, 2013, 81, 12-28.	3.0	46
88	Pliocene orographic barrier uplift in the southern Central Andes. Geology, 2014, 42, 691-694.	4.4	46
89	Tectonoâ€sedimentary evolution of the northern Iranian Plateau: insights from middle–late Miocene forelandâ€basin deposits. Basin Research, 2017, 29, 417-446.	2.7	46
90	Response of the East African climate to orbital forcing during the last interglacial (130–117 ka) and the early last glacial (117–60 ka). Geology, 2001, 29, 499.	4.4	45

#	Article	IF	CITATIONS
91	Style and evolution of salt pillows and related structures in the northern part of the Northeast German Basin. International Journal of Earth Sciences, 2000, 89, 652-664.	1.8	44
92	Tectonic control on rock uplift, exhumation, and topography above an oceanic ridge collision: Southern Patagonian Andes (47°S), Chile. Tectonics, 2016, 35, 1317-1341.	2.8	43
93	Late Miocene–early Pliocene onset of N–S extension along the southern margin of the Central Andean Puna Plateau: Evidence from magmatic, geochronological and structural observations. Tectonophysics, 2010, 494, 48-63.	2.2	42
94	Sea level and climate forcing of the Sr isotope composition of late <scp>M</scp> iocene <scp>M</scp> editerranean marine basins. Geochemistry, Geophysics, Geosystems, 2014, 15, 2964-2983.	2.5	42
95	Rapid Last Glacial Maximum deglaciation in the Indian Himalaya coeval with midlatitude glaciers: New insights from ¹⁰ Beâ€dating of iceâ€polished bedrock surfaces in the Chandra Valley, NW Himalaya. Geophysical Research Letters, 2016, 43, 1589-1597.	4.0	42
96	Landscape response to late Pleistocene climate change in NW Argentina: Sediment flux modulated by basin geometry and connectivity. Journal of Geophysical Research F: Earth Surface, 2016, 121, 392-414.	2.8	42
97	Controls on submarine canyon activity during sea-level highstands: The BiobÃo canyon system offshore Chile. , 2015, 11, 1226-1255.		40
98	Pronounced increase in slope instability linked to global warming: A case study from the eastern European Alps. Earth Surface Processes and Landforms, 2021, 46, 1328-1347.	2.5	40
99	The stable isotope altimeter: Do Quaternary pedogenic carbonates predict modern elevations?. Geology, 2009, 37, 1015-1018.	4.4	39
100	Steady rifting in northern Kenya inferred from deformed Holocene lake shorelines of the Suguta and Turkana basins. Earth and Planetary Science Letters, 2012, 331-332, 335-346.	4.4	37
101	Neogene paleoelevation of intermontane basins in a narrow, compressional mountain range, southern Central Andes of Argentina. Earth and Planetary Science Letters, 2014, 406, 153-164.	4.4	37
102	Surface uplift and convective rainfall along the southern Central Andes (Angastaco Basin, NW) Tj ETQq0 0 0 rgBT	Qverlock	2 1 <u>0</u> Tf 50 30
103	Holocene internal shortening within the northwest Subâ€Himalaya: Outâ€ofâ€sequence faulting of the Jwalamukhi Thrust, India. Tectonics, 2016, 35, 2677-2697.	2.8	36
104	Volcano-tectonic evolution of the Chyulu Hills and implications for the regional stress field in Kenya. Geology, 1995, 23, 165.	4.4	33
105	Rainfall variability and trends of the past six decades (1950–2014) in the subtropical NW Argentine Andes. Climate Dynamics, 2017, 48, 1049-1067.	3.8	33
106	Victoria continental microplate dynamics controlled by the lithospheric strength distribution of the East African Rift. Nature Communications, 2020, 11, 2881.	12.8	33
107	Quaternary Depositional Systems in Northern Lake Baikal, Siberia. Journal of Geology, 1999, 107, 1-12.	1.4	31

108 TerraceM: A MATLAB® tool to analyze marine and lacustrine terraces using high-resolution topography. , 2016, 12, 176-195.

 $\mathbf{31}$

#	Article	IF	CITATIONS
109	Lake overspill and onset of fluvial incision in the Iranian Plateau: Insights from the Mianeh Basin. Earth and Planetary Science Letters, 2017, 469, 135-147.	4.4	31
110	Tectonic implications of fluvial incision and pediment deformation at the northern margin of the Central Anatolian Plateau based on multiple cosmogenic nuclides. Tectonics, 2013, 32, 1107-1120.	2.8	30
111	Elevation-dependent changes in n -alkane δD and soil GDGTs across the South Central Andes. Earth and Planetary Science Letters, 2016, 453, 234-242.	4.4	29
112	Quantifying offshore foreâ€ e rc deformation and splayâ€fault slip using drowned Pleistocene shorelines, Arauco Bay, Chile. Journal of Geophysical Research: Solid Earth, 2017, 122, 4529-4558.	3.4	29
113	Recurrence of Large Earthquakes in Magmatic Continental Rifts: Insights from a Paleoseismic Study along the Laikipia-Marmanet Fault, Subukia Valley, Kenya Rift. Bulletin of the Seismological Society of America, 2009, 99, 61-70.	2.3	28
114	Cenozoic extension in the Kenya Rift from lowâ€ŧemperature thermochronology: Links to diachronous spatiotemporal evolution of rifting in East Africa. Tectonics, 2015, 34, 2367-2386.	2.8	28
115	Shelfal sediment transport by an undercurrent forces turbidity-current activity during high sea level along the Chile continental margin. Geology, 2016, 44, 295-298.	4.4	28
116	Sedimentary loading–unloading cycles and faulting in intermontane basins: Insights from numerical modeling and field observations in the NW Argentine Andes. Earth and Planetary Science Letters, 2019, 506, 388-396.	4.4	28
117	Timing of past glaciation at the Sierra de Aconquija, northwestern Argentina, and throughout the Central Andes. Quaternary Science Reviews, 2019, 204, 37-57.	3.0	28
118	Asymmetric late Pleistocene glaciations in the North Basin of the Baikal Rift, Russia. Journal of the Geological Society, 1998, 155, 61-69.	2.1	27
119	Short-lived increase in erosion during the African Humid Period: Evidence from the northern Kenya Rift. Earth and Planetary Science Letters, 2017, 459, 58-69.	4.4	27
120	Turbidite paleoseismology along the active continental margin of Chile – Feasible or not?. Quaternary Science Reviews, 2015, 120, 71-92.	3.0	26
121	Spatio-temporal trends in normal-fault segmentation recorded by low-temperature thermochronology: Livingstone fault scarp, Malawi Rift, East African Rift System. Earth and Planetary Science Letters, 2016, 455, 62-72.	4.4	26
122	Controls on intermontane basin filling, isolation and incision on the margin of the Puna Plateau, <scp>NW</scp> Argentina (~23ŰS). Basin Research, 2017, 29, 131-155.	2.7	26
123	Sedimentary evidence for late Messinian uplift of the <scp>SE</scp> margin of the Central Anatolian Plateau: Adana Basin, southern Turkey. Basin Research, 2017, 29, 488-514.	2.7	25
124	Multiple Exhumation Phases in the Central Pontides (N Turkey): New Temporal Constraints on Major Geodynamic Changes Associated With the Closure of the Neoâ€Tethys Ocean. Tectonics, 2018, 37, 1831-1857.	2.8	25
125	Late Cenozoic topographic evolution of the Eastern Cordillera and Puna Plateau margin in the southern Central Andes (NW Argentina). Earth and Planetary Science Letters, 2020, 535, 116112.	4.4	25
126	Repeated largeâ€magnitude earthquakes in a tectonically active, lowâ€strain continental interior: The northern Tien Shan, Kyrgyzstan. Journal of Geophysical Research: Solid Earth, 2016, 121, 3888-3910.	3.4	24

#	Article	IF	CITATIONS
127	Immediate propagation of deglacial environmental change to deep-marine turbidite systems along the Chile convergent margin. Earth and Planetary Science Letters, 2017, 473, 190-204.	4.4	24
128	Late Cenozoic tectonics and denudation in the Central Kenya Rift: quantification of long-term denudation rates. Tectonophysics, 1997, 278, 83-94.	2.2	23
129	The topographic imprint of a transient climate episode: the western Andean flank between 15·5° and 41·5°S. Earth Surface Processes and Landforms, 2010, 35, 1516-1534.	2.5	23
130	Synsedimentary brokenâ€foreland tectonics during the Paleogene in the Andes of NW Argentine: new evidence from regional to centimetreâ€scale deformation features. Basin Research, 2018, 30, 142-159.	2.7	22
131	Effects of deepâ€seated versus shallow hillslope processes on cosmogenic ¹⁰ Be concentrations in fluvial sand and gravel. Earth Surface Processes and Landforms, 2018, 43, 3086-3098.	2.5	22
132	TerraceM-2: A Matlab® Interface for Mapping and Modeling Marine and Lacustrine Terraces. Frontiers in Earth Science, 2019, 7, .	1.8	22
133	The Frolikha Fan; a large Pleistocene glaciolacustrine outwash fan in northern Lake Baikal, Siberia. Journal of Sedimentary Research, 1998, 68, 841-849.	1.6	22
134	Assessing tectonic and climatic causal mechanisms in forelandâ€basin stratal architecture: insights from the Alborz Mountains, northern Iran. Earth Surface Processes and Landforms, 2014, 39, 110-125.	2.5	21
135	Late Pleistocene Climate Change and Erosion in the Santa Maria Basin, NW Argentina. Journal of Sedimentary Research, 2003, 73, 82-90.	1.6	19
136	The Mid-Miocene East African Plateau: a pre-rift topographic model inferred from the emplacement of the phonolitic Yatta lava flow, Kenya. Geological Society Special Publication, 2011, 357, 285-300.	1.3	19
137	Quaternary uplift of the northern margin of the Central Anatolian Plateau: New OSL dates of fluvial and delta-terrace deposits of the Kızılırmak River, Black Sea coast, Turkey. Quaternary Science Reviews, 2018, 201, 446-469.	3.0	19
138	Episodic out-of-sequence deformation promoted by Cenozoic fault reactivation in NW Argentina. Tectonophysics, 2020, 776, 228276.	2.2	19
139	Segmented seismicity of the M w 6.2 Baladeh earthquake sequence (Alborz Mountains, Iran) revealed from regional moment tensors. Journal of Seismology, 2013, 17, 925-959.	1.3	18
140	Local high relief at the southern margin of the Andean plateau by 9ÂMa: evidence from ignimbritic valley fills and river incision. Terra Nova, 2014, 26, 454-460.	2.1	18
141	Climatic controls on debrisâ€flow activity and sediment aggradation: The Del Medio fan, NW Argentina. Journal of Geophysical Research F: Earth Surface, 2016, 121, 2424-2445.	2.8	18
142	Riverâ€discharge dynamics in the Southern Central Andes and the 1976–77 global climate shift. Geophysical Research Letters, 2016, 43, 11,679.	4.0	18
143	Oscillations and trends of river discharge in the southern Central Andes and linkages with climate variability. Journal of Hydrology, 2017, 555, 108-124.	5.4	18
144	Fast Holocene slip and localized strain along the Liquiñe-Ofqui strike-slip fault system, Chile. Scientific Reports, 2021, 11, 5970.	3.3	18

#	Article	IF	CITATIONS
145	Structural and chemical evolution of pseudotachylytes during seismic events. Mineralogy and Petrology, 1996, 58, 33-50.	1.1	17
146	Luminescence dating of alluvial fans in intramontane basins of NW Argentina. Geological Society Special Publication, 2005, 251, 153-168.	1.3	17
147	Slip along the Sultanhanı Fault in Central Anatolia from deformed Pleistocene shorelines of palaeo-lake Konya and implications for seismic hazards in low-strain regions. Geophysical Journal International, 2017, 209, 1431-1454.	2.4	17
148	Interactions between main channels and tributary alluvial fans: channel adjustments and sediment-signal propagation. Earth Surface Dynamics, 2020, 8, 303-322.	2.4	16
149	Miocene to Quaternary basin evolution at the southeastern Andean Plateau (Puna) margin (ca. 24°S) Tj ETQq1	1	4 ggBT /Over
150	Controls on Asymmetric Rift Dynamics: Numerical Modeling of Strain Localization and Fault Evolution in the Kenya Rift. Tectonics, 2021, 40, e2020TC006553.	2.8	15
151	Historical coseismic surface deformation of fluvial gravel deposits, Schafberg fault, Lower Rhine Graben, Germany. International Journal of Earth Sciences, 2018, 107, 571-585.	1.8	14
152	Segmentation of the Main Himalayan Thrust Revealed by Lowâ€Temperature Thermochronometry in the Western Indian Himalaya. Tectonics, 2018, 37, 2710-2726.	2.8	14
153	Deepâ€seated gravitational slope deformation (DSCSD) and slowâ€moving landslides in the southern Tien Shan Mountains: new insights from InSAR, tectonic and geomorphic analysis. Earth Surface Processes and Landforms, 2019, 44, 2333-2348.	2.5	14
154	Continental rifting at magmatic centres: structural implications from the Late Quaternary Menengai Caldera, central Kenya Rift. Journal of the Geological Society, 2020, 177, 153-169.	2.1	14
155	Development of an incipient Paleogene topography between the presentâ€day Eastern Andean Plateau (Puna) and the Eastern Cordillera, southern Central Andes, NW Argentina. Basin Research, 2021, 33, 1194-1217.	2.7	14
156	Pliocene–Pleistocene orographic control on denudation in northwest Argentina. Geology, 2019, 47, 359-362.	4.4	13
157	Glacial morphology in the Chinese Pamir: Connections among climate, erosion, topography, lithology and exhumation. Geomorphology, 2014, 221, 1-17.	2.6	12
158	Stratigraphic architecture of the upper Messinian deposits of the Adana Basin (Southern Turkey): implications for the Messinian salinity crisis and the Taurus petroleum system. Italian Journal of Geosciences, 2016, 135, 408-424.	0.8	12
159	Variability of the geothermal gradient across two differently aged magma-rich continental rifted margins of the Atlantic Ocean: the Southwest African and the Norwegian margins. Solid Earth, 2018, 9, 139-158.	2.8	12
160	Late Quaternary tectonics controlled by fault reactivation. Insights from a local transpressional system in the intermontane Lerma valley, Cordillera Oriental, NW Argentina. Journal of Structural Geology, 2019, 128, 103875.	2.3	12
161	Lithospheric density structure of the southern Central Andes constrained by 3D data-integrative gravity modelling. International Journal of Earth Sciences, 2021, 110, 2333-2359.	1.8	12
162	Crustal Structure of the Andean Foreland in Northern Argentina: Results From Dataâ€Integrative Threeâ€Dimensional Density Modeling. Journal of Geophysical Research: Solid Earth, 2018, 123, 1875-1903.	3.4	11

#	Article	IF	CITATIONS
163	Neotectonic Activity in the Low-Strain Broken Foreland (Santa BÃjrbara System) of the North-Western Argentinean Andes (26°S). Lithosphere, 2020, 2020, .	1.4	11
164	Distribution of Temperature and Strength in the Central Andean Lithosphere and Its Relationship to Seismicity and Active Deformation. Journal of Geophysical Research: Solid Earth, 2021, 126, e2020JB021231.	3.4	11
165	Paleoseismic Record of Three Holocene Earthquakes Rupturing the Issykâ€Ata Fault near Bishkek, North Kyrgyzstan. Bulletin of the Seismological Society of America, 2017, 107, 2721-2737.	2.3	10
166	Hidden Holocene Slip Along the Coastal El Yolki Fault in Central Chile and Its Possible Link With Megathrust Earthquakes. Journal of Geophysical Research: Solid Earth, 2019, 124, 7280-7302.	3.4	10
167	Marine terraces of the last interglacial period along the Pacific coast of South America (1º N–40º S). Earth System Science Data, 2021, 13, 2487-2513.	9.9	10
168	Longâ€Term Lithospheric Strength and Upperâ€Plate Seismicity in the Southern Central Andes, 29°–39°S. Geochemistry, Geophysics, Geosystems, 2022, 23, .	2.5	10
169	Active faulting in a populated low-strain setting (Lower Rhine Graben, Central Europe) identified by geomorphic, geophysical and geological analysis. Geological Society Special Publication, 2017, 432, 127-146.	1.3	8
170	The influence of variations in crustal composition and lithospheric strength on the evolution of deformation processes in the southern Central Andes: insights from geodynamic models. International Journal of Earth Sciences, 2021, 110, 2361-2384.	1.8	8
171	3-D crustal density model of the Sea of Marmara. Solid Earth, 2019, 10, 785-807.	2.8	7
172	Temperature and precipitation in the southern Central Andes during the last glacial maximum, Heinrich Stadial 1, and the Younger Dryas. Quaternary Science Reviews, 2020, 248, 106592.	3.0	7
173	Validation and calibration of soil Î'2H and brGDGTs along (E-W) and strike (N-S) of the Himalayan climatic gradient. Geochimica Et Cosmochimica Acta, 2020, 290, 408-423.	3.9	6
174	Quantifying Tectonic and Glacial Controls on Topography in the Patagonian Andes (46.5°S) From Integrated Thermochronometry and Thermoâ€Kinematic Modeling. Journal of Geophysical Research F: Earth Surface, 2021, 126, e2020JF005993.	2.8	6
175	The Pamir Frontal Thrust Fault: Holocene Fullâ€6egment Ruptures and Implications for Complex Segment Interactions in a Continental Collision Zone. Journal of Geophysical Research: Solid Earth, 2021, 126, e2021JB022405.	3.4	6
176	Impact of Late Pleistocene climate variability on paleo-erosion rates in the western Himalaya. Earth and Planetary Science Letters, 2022, 578, 117326.	4.4	5
177	Sediment provenance and silicic volcano-tectonic evolution of the northern East African Rift System from U/Pb and (U-Th)/He laser ablation double dating of detrital zircons. Earth and Planetary Science Letters, 2022, 580, 117375.	4.4	5
178	Identification of Debrisâ€Flow Channels Using Highâ€Resolution Topographic Data: A Case Study in the Quebrada del Toro, NW Argentina. Journal of Geophysical Research F: Earth Surface, 2021, 126, e2021JF006330.	2.8	4
179	The cryptic seismic potential of the Pichilemu blind fault in Chile revealed by off-fault geomorphology. Nature Communications, 2022, 13, .	12.8	4
180	Reply to Giresse et al.: No evidence for climate variability during the late Holocene rainforest crisis in Western Central Africa. Proceedings of the National Academy of Sciences of the United States of America, 2018, 115, E6674-E6675.	7.1	3

#	Article	IF	CITATIONS
181	Reply to Clist et al.: Human activity is the most probable trigger of the late Holocene rainforest crisis in Western Central Africa. Proceedings of the National Academy of Sciences of the United States of America, 2018, 115, E4735-E4736.	7.1	3
182	Midâ€Pleistocene to Recent Crustal Extension in the Inner Graben of the Northern Kenya Rift. Geochemistry, Geophysics, Geosystems, 2022, 23, .	2.5	3
183	Geomorphic expression of a tectonically active rift-transfer zone in southern Ethiopia. Geomorphology, 2022, 403, 108162.	2.6	3
184	Controls of the Lithospheric Thermal Field of an Ocean-Continent Subduction Zone: The Southern Central Andes. Lithosphere, 2022, 2022, .	1.4	3
185	Late Pleistocene to Recent Deformation in the Thickâ€Skinned Foldâ€andâ€Thrust Belt of Northwestern Argentina (Central CalchaquÃ-Valley, 26°S). Tectonics, 2021, 40, e2020TC006394.	2.8	2
186	Lithospheric strength variations and seismotectonic segmentation below the Sea of Marmara. Tectonophysics, 2021, 815, 228999.	2.2	2
187	Corrigendum to "Role of climate and vegetation density in modulating denudation rates in the Himalaya―[Earth Planet. Sci. Lett. 445 (2016) 57–67]. Earth and Planetary Science Letters, 2020, 540, 116252.	4.4	1
188	Local effects on soil leaf wax hydrogen isotopes along a west to east transect through the Pamirs, Tajikistan. Organic Geochemistry, 2021, 160, 104272.	1.8	1
189	Glacial Catchment Erosion From Detrital Zircon (Uâ€Th)/He Thermochronology: Patagonian Andes. Journal of Geophysical Research F: Earth Surface, 2021, 126, e2021JF006141.	2.8	1
190	Tectonic and sediment supply control of deep rift lake turbidite systems: Lake Baikal, Russia: Comment and Reply. Geology, 2000, 28, 189-191.	4.4	1
191	Present-day E-W extension in the NW Himalaya (Himachal Pradesh, India). Himalayan Journal of Sciences, 2008, 5, 67-68.	0.3	0
192	Corrigendum to "Short-lived increase in erosion during the African Humid Period: Evidence from the northern Kenya Rift―[Earth Planet. Sci. Lett. 459 (2017) 58–69]. Earth and Planetary Science Letters, 2017, 474, 528.	4.4	0
193	From Proterozoic tectonics to Quaternary climate variability: Earth system science studies in Latin America. International Journal of Earth Sciences, 2021, 110, 2269-2271.	1.8	0